CARBON 49 (2011) 4280–4290

available at www.sciencedirect.com

ScienceDirect

journal homepage: www.elsevier.com/locate/carbon

The effect of filler type and content and the manufacturing process on the performance of multifunctional carbon/poly-lactide composites

Massimiliano Tait [a,b], *Alessandro Pegoretti* [b], *Andrea Dorigato* [b], *Kyriaki Kalaitzidou* [a,c,*]

[a] *George Woodruff School of Mechanical Engineering, Georgia Institute of Technology, Atlanta, GA 30322, USA*
[b] *Department of Materials Engineering and Industrial Technologies, University of Trento, Italy*
[c] *School of Materials Science and Engineering, Georgia Institute of Technology, Atlanta, GA 30322, USA*

ARTICLE INFO

Article history:
Received 8 September 2010
Accepted 2 June 2011
Available online 12 June 2011

ABSTRACT

Two nanosized carbonaceous fillers, vapor grown carbon nanofibers and exfoliated graphite nanoplatelets, were used to prepare poly(lactide acid) composites at various concentrations from 0 up to 20 wt.%. The two fillers were also combined in order to explore possible synergistic actions. Two compounding processes, melt mixing and polymer dissolution, and two forming methods, injection and compression molding, were used to manufacture the composites. The flexural properties, impact strength, storage and loss modulus, Vicat softening temperature, and electrical conductivity of neat matrix and composites were determined as a function of the filler type and content, and of the processing method used. The filler dispersion within the polymer matrix, the presence of agglomerates and the existence of voids were studied using field-emission scanning electron microscopy. It is concluded that compounding by polymer dissolution followed by compression molding leads to composites with the lowest percolation threshold and surface conductivity and highest storage modulus whereas extrusion injection molding results in composites with the highest mechanical properties. The results can be used to engineer biodegradable composites with specific properties for targeted applications.

1. Introduction

Polymers reinforced with nano-sized fillers are promising candidates for various applications requiring lightweight and high-performance, multifunctional materials. The basic characteristics of nano-sized materials that are responsible for their unique properties are the nanometer length scales and enormously large surface area-to-volume ratio. These features can enhance the overall material performance by synergistically producing unique properties resulting from phenomena that occur only when the morphology and the physics coincide at the nanoscale [1]. The main challenges in utilizing these materials as polymer fillers are to control and optimize their dispersion within the polymer matrix and their interface chemistry [2–5], and maintain their nanoscale morphology during the manufacturing process [6].

In addition to the filler and manufacturing process employed to fabricate the composites, the resulting properties strongly depend on the polymer used as matrix. Petroleum based polymers such as polypropylene [4,6], nylons [7], polystyrene [8] and epoxies [5] have commonly been used but due to the increased trend for environmentally friendly materials, biodegradable polymers from renewable resources such as poly(lactide) acid (PLA) have become very popular. Land fill

---

[*] *Corresponding author at:* George Woodruff School of Mechanical Engineering, Georgia Institute of Technology, Atlanta, GA 30322, USA. Fax: +1 404 894 9342.

E-mail address: kyriaki.kalaitzidou@me.gatech.edu (K. Kalaitzidou).

0008-6223/$ - see front matter © 2011 Elsevier Ltd. All rights reserved.
doi:10.1016/j.carbon.2011.06.009

or recycle are not viable solutions because the first one is a temporary measure and the second is energy insufficient and leads to downgrade of the materials.

PLA is a renewable, biodegradable and eco-friendly thermoplastic polyester with properties comparable, if not better, to those of petroleum based polyolefins [9–11]. It possesses relatively high melting point [12], and can exhibit good mechanical performances [13]. PLA based composites have successfully been made and characterized using various nano-sized fillers including electrically conductive materials such as carbon nanotubes (CNTs) [14,15], expanded graphite [16] and exfoliated graphite [17,18].

The advantage of using electrically and thermally conductive nano-sized fillers is that they result in light weight, relatively low cost and easily processed composites with enhanced overall performance. Such multifunctional composites can be used in a wide range of applications including but not limited to energy harvesting, flexible electronics, thermal interphase materials and structural components for automotive and aerospace vehicles. CNTs exhibit superior mechanical, thermal and electrical properties [19] but their use as polymer reinforcements for engineering applications is currently cost prohibitive. Exfoliated graphite nanoplatelets, xGnPs™, have the same chemistry and thus exhibit the same properties as CNTs, with the basic difference that xGnPs have a layered structure instead of tubular. Polymers reinforced with CNTs usually show lower percolation threshold, i.e., the amount of CNTs to induce conductivity, due to their fiber like shape and high aspect ratio. xGnPs provide multifunctionality in polymers like polypropylene [20] but there are no comprehensive studies on the effect of xGnPs on the overall performance of PLA. Vapor grown carbon fibers (VGCFs) have similar chemistry with CNTs, cost significantly less and are commonly used as reinforcements for polymers.

Several scientific studies can be found on the potential of various carbon based nanofillers in increasing both the mechanical and the electrical properties of polymer matrices. However, information on the effects of the manufacturing process on the multifunctional properties of the prepared composites are relatively scarce in the open scientific literature. Therefore, the main aim of the present work is to provide a contribution for the comprehension of the relationships between the manufacturing processes, the microstructural features and the final mechanical and electrical properties in xGnP/PLA and VGCF/PLA composites. Both xGnPs and VGCFs are potential alternatives for CNTs. Furthermore, synergistic effects between nanofillers on the mechanical and electrical properties of the resulting composites have been investigated. This work can lead to fabrication of biodegradable composites with engineered electrical conductivity and mechanical performance which can be achieved by tuning the processing-property relationship.

2. Experimental

2.1. *Materials*

Poly(lactic acid) (PLA, MW = 1.42×10^4 g/mol, pellets, semi crystalline) was purchased from Nature Works LLC, Minnetonka, Minnesota, USA (product code 3051D). VGCFs were purchased from Pyrograf Products Inc., Cedarville, Ohio (product code PR.19.XT.LHT). According to the manufacturer, the diameter of the fibers ranges from 100 to 200 nm, while the length is within 30–100 μm and the specific surface area is about 20–30 m^2/g. xGnPs™ with an average diameter of about 15–25 μm, a thickness in the range of 10–20 nm, and a specific surface area of about 50–80 m^2/g were supplied by XG Sciences, East Lansing, Michigan (product code B006-1). The methylene chloride used for dissolving the PLA was purchased from VWR International LCC, Atlanta, Georgia.

2.2. *Fabrication of composites*

2.2.1. *Extrusion – injection molding (EX-IM)*

PLA, VGCFs and xGnPs at predetermined loadings were melt mixed and injection molded. A vertical, co-rotating, bench top twin screw micro-extruder (DSM Micro 15cc Compounder) connected to a micro-injection molding unit (DSM) were used. The polymer was mixed with the fillers for 2.5 min, at 180 °C and a screw speed of 150 rpm. The temperature of the mold was 80 °C, and the injection molding pressure about 8 bar. PLA composites containing from 0 to 20 wt.% of VGCFs or xGnPs were made. In addition, composites containing both fillers up to 20 wt.% of total filler loading at various VGCF:xGnP ratios were also made to investigate possible synergy effects between fillers on the properties of the PLA based composites. Prior to testing and characterization the samples were stored at room temperature in sealed plastic bags.

2.2.2. *Extrusion – compression molding (EX-CM)*

Composite pellets made by melt mixing PLA with the fillers and pelletizing the extrudate were used for compression molding. The twin screw extruder operating at the conditions mentioned above was used for melt mixing and the rod-shape extrudate with an average diameter of 1 mm was cut in pellets with length in the range of 3–4 mm. A four-column manual hydraulic press (CARVER, model 3855, 25 ton), a custom-made steel mold and aluminum plates, used to avoid contamination of the press platens by the melt, were employed for compression molding. A Teflon fabric was also used to allow removal of the composite specimens from the mold. The mold filled with the composite pellets was placed in the hot press which was preheated at 195 °C. No pressure was applied for 5 min to assure that the pellets melt without being plastically deformed. Then a pressure of 5.87 MPa was applied for 10 min. Finally, the mold was removed from the hot press and air-cooled from 195 °C to ambient temperature under a pressure of 0.02 MPa to avoid warpage. Upon completion of cooling the composite sheets were stored in sealed plastic bags.

2.2.3. *Solution – compression molding (SO-CM)*

In case of VGCF/PLA composites, PLA pellets were soaked in methylene chloride (19 g of PLA in 200 ml of solvent) for 15 min at ambient temperature. Predetermined amount of VGCFs were added to the solution which was magnetically stirred at 200 rpm for 8 h at ambient temperature. The solvent was evaporated through drying under a hood for 24 h. The resulting composite sheets were pelletized and used for compression molding. To facilitate dispersion, in case of xGnP/PLA composites pre-weighted amount of xGnPs was dispersed in 500 ml of methylene chloride using a sonication probe (Misonix 6000, 12.5 mm diameter, 50% amplitude, 30 W power) for 10 min. Then PLA pellets were added to the xGnP solution (19 g PLA in 500 ml of solvent) and the procedure of magnetic stirring and evaporation of the solvent used in case of VGCF/PLA was followed. The only difference in case of xGnP is that evaporation of the solvent was allowed for 32 instead of 24 h due to the larger amount of solvent used. The obtained xGnP/PLA film was pelletized and compression molded using the equipment and conditions described above. Upon completion of cooling, the composite sheets were stored in sealed plastic bags.

2.3. *Testing and characterization of composites*

2.3.1. *Mechanical and thermomechanical testing*

The flexural properties of the PLA composites were determined by three point bending test according to ASTM D790 standard performed using a universal mechanical testing machine, MTI INSTRON. The tests were carried out at a crosshead speed of 1.27 mm/min, and a support span-to-depth ratio of at least 16:1 was adopted. Due to the different cross-section of the specimens, a preload of 22.2 and 2.22 N was applied for the composites made by IM and CM, respectively.

Charpy impact tests were performed according to ASTM D6110 standard by a CEAST instrumented pendulum at an impact speed and energy of 3.46 m/s and 2 J, respectively. Rectangular notched specimens, 63 mm long, 12.7 mm wide and 3.3 mm thick were utilized, setting a span length of 40 mm. The depth and tip-radius of the notch were 2.5 and 0.25 mm, respectively. At least three specimens were tested for each sample.

The dynamic-mechanical properties, including storage and loss modulus and tanδ, were determined as a function of temperature using a DMA Q800 (TA Instruments) apparatus in tensile configuration. The conditions used were clamp distance of 11.5 mm, 1 Hz frequency, 0.01 N preload, and strain amplitude of 64 μm. The specimens were cooled down and equilibrated for 5 min at 0 °C and then heated at a rate of 3 °C/min up to 100 °C.

The determination of the Vicat softening temperature was performed utilizing a HDT-Vicat mod. MP/3 (ATS FAAR) apparatus, according to ASTM D1525-07 standard. The parameters used were: load 10 N, initial temperature 30 °C, heating rate 50 °C/h. The dimensions of the samples were: thickness 3.3 mm, length 12.7 mm, width 7 mm.

2.3.2. *Electrical conductivity and morphological characterization of PLA composites*

The surface resistivity of the PLA composites was determined as a function of the filler type, content and manufacturing process based on the four probe method in a frequency range of 10^2–10^5 Hz using a SI 1287 electrochemical interface Solatron applying a voltage of 400 mV.

The morphology of the fracture surfaces of neat PLA and composite specimens was observed by a Zeiss Supra40 field-emission scanning electron microscope (FESEM), at an acceleration voltage of 4 kV. Specimens were cryofractured in liquid nitrogen and then metallized before the observations.

3. Results and discussion

3.1. *Flexural properties*

Representative stress–strain curves of VGCF/PLA composites obtained by EX-IM as a function of the VGCF content are shown in Fig. 1. The data reported is the average of five tests. As indicated, addition of VGCFs drastically increases the flexural modulus and decreases the ultimate strain, whereas increase in the flexural strength observed only for VGCF loading above 10 wt.% is within experimental error, i.e., 8% higher than the strength of the neat PLA and is not considered statistically significant. Details on the effect of VGCFs on the flexural strength of PLA are provided below in the discussion of Fig. 5.

The stress–strain plots of xGnP/PLA composites made by EX-IM are shown in Fig. 2. In this case, the addition of xGnPs

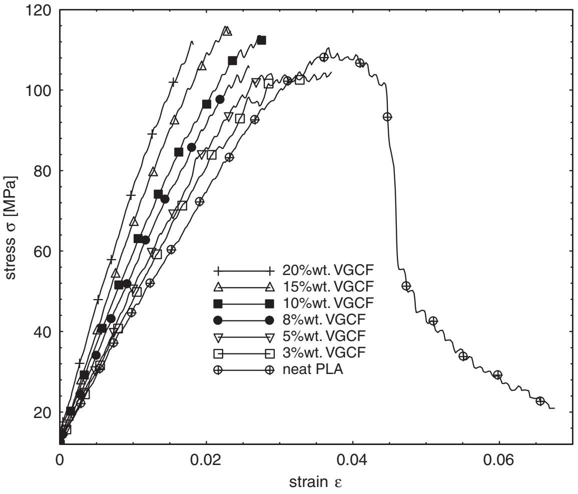

Fig. 1 – Stress–strain curves of VGCF/PLA composites made by EX-IM process.

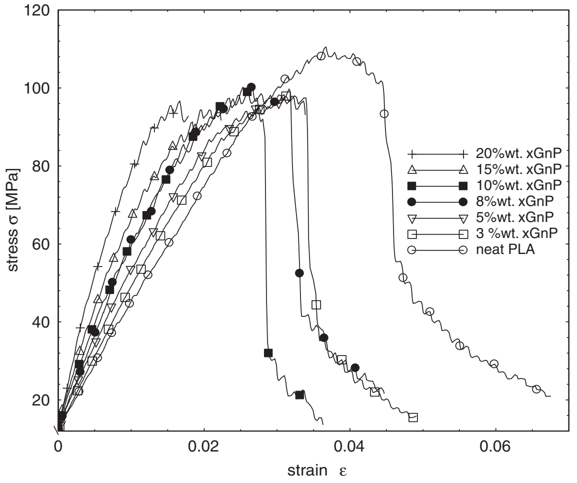

Fig. 2 – Stress–strain curves for xGnP/PLA composites made by EX-IM.

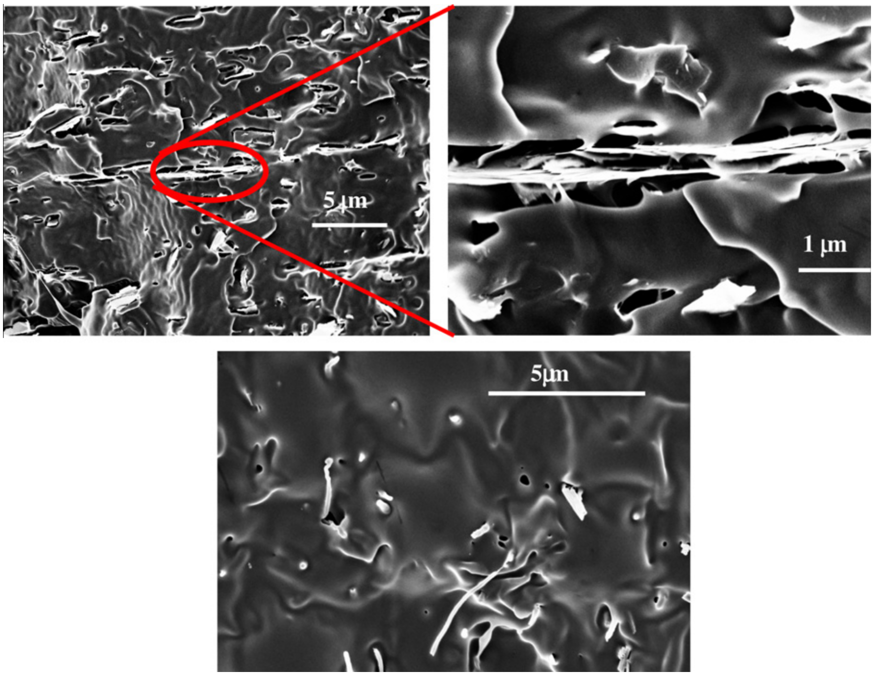

Fig. 3 – FESEM images of the fracture surfaces of (a and b) 3 wt.% xGnP/PLA nanocomposites made by EX-IM, showing voids at the xGnP/PLA interface, and (c) 3 wt.% VGCF/PLA nanocomposite.

increases the modulus but reduces the flexural strength for any of the xGnP loadings used in this study. The decrease in strength indicates either poor dispersion of the fillers, presence of agglomerates or existence of defects such as voids as shown in the SEM images presented inFig. 3a and b. Imperfect xGnP/PLA contact at the interface due to poor interactions results in insufficient stress transfer and thus decrease in strength. It is worthwhile to observe that PLA is hydrophilic and thus xGnP which has no functional groups tends to form agglomerates within the polymer. Similar microstructural features, such as voids around the nanofibers and holes in the polymer matrix caused by poor fiber–polymer interactions and fiber/matrix debonding, are also observed in the VGCF/PLA EX-IM composite, shown in Fig. 3c. The lack of functional groups in VGCFs is responsible for the weak interfacial adhesion. However, xGnPs due to their higher surface area tend to aggregate more than VGCFs do, which may be the reason for the strength decrease upon addition of xGnP. This hypothesis is also supported by Fig. 3c showing VGCFs dispersed better within the matrix compared to xGnPs shown in Fig. 3a and b.

The effect of filler, type and content, and processing method on the flexural modulus and strength of xGnP or VGCF reinforced PLA composites is summarized in Figs. 4 and 5, respectively. The processing methods considered are EX-IM and EX-CM. It is expected that IM will lead to filler alignment along the injection direction especially in the case of VGCF which have high aspect ratio. Such alignment could result in higher tensile modulus and strength values because the direction of the applied load in tensile testing is along the fiber axis. However, it is not clear what impact the filler alignment will have on the flexural properties. Usually composites made by CM are not as highly packed and contain more defects including microvoids compared to composites made by IM. However, CM leads to composites with random filler distribution which means lower percolation threshold, in case of electrically conductive fillers. Thus it is of main importance to determine the optimum processing method which combined with the proper filler can lead to composites with the best overall performance.

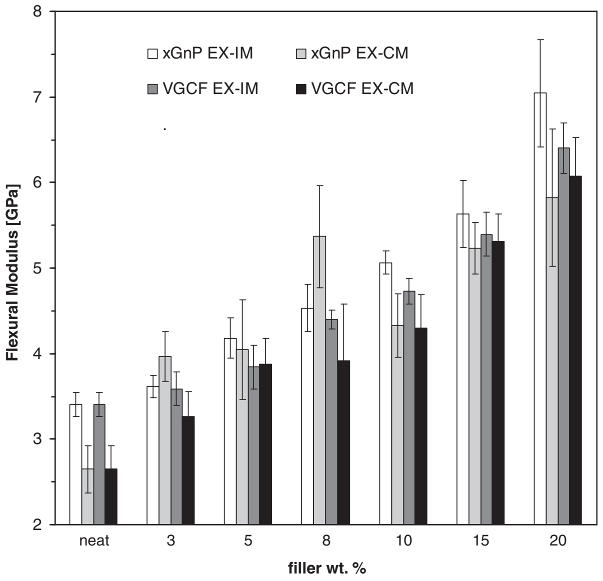

Fig. 4 – Effect of filler and processing method on the flexural modulus of PLA composites.

As indicated in Fig. 4, the flexural modulus of neat PLA specimens made by CM is about 30% lower compared to the modulus of PLA specimens made by IM. However, this difference becomes less significant upon addition of xGnPs

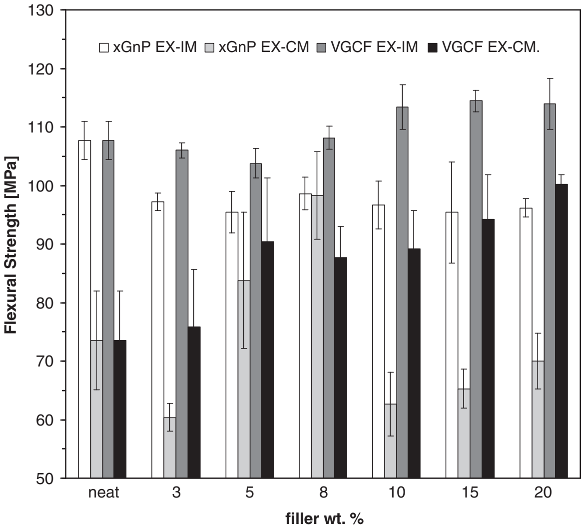

Fig. 5 – Effect of filler type and content, and processing method on the flexural strength of PLA composites.

or VGCFs. It is noted that the results presented in Fig. 4 are not conclusive due to large standard deviations and overlapping of error bars. The large standard deviation values are mainly attributed to the lack of a homogeneous distribution of nanofiller aggregates and/or in the presence of aggregates of different size, a result of the compounding methods employed and the processing conditions used. Overall, xGnP increases the modulus more than VGCF do at the same filler content.

As shown in Fig. 5, CM leads to PLA specimens with roughly 40% lower flexural strength than those made by IM. This result is also supported by the morphology of the fracture surfaces of PLA specimens made by IM and CM reported in Fig. 6a and b, respectively. The fracture surface of the injection molded specimen is rougher, thus indicating larger energy adsorption during testing. Addition of xGnPs decreases the strength, for all xGnP loadings used, in case of IM whereas in case of CM the strength unexpectedly increases for 5 and 8 wt.% of xGnP. In general, the poor strength of xGnP/PLA could be probably attributed to weak xGnP/polymer interactions. In case of VGCF/PLA composites made by IM the strength increases only at VGCF loading higher than 8 wt.% whereas, improvement in strength is observed for all VGCF loadings used when CM is used.

The unexpectedly high modulus (Fig. 4) and strength (Fig. 5) of the 5% and 8% of xGnP composite made by EX-CM is probably due to random variation in processing conditions such as screw speed (rpm) during melt mixing in the extruder or to cross contamination of the screws. Another possible reason for the large values of standard deviation can be probably attributed to an irregular distribution of nanofiller aggregates. Furthermore, the effect of the manufacturing process and of the processing conditions have to be taken into account. As it will be shown in Fig. 14, in EX-CM composites VGCFs are randomly and homogeneously dispersed within the matrix and thus the strength of the resulting composites progressively increases with the VGCF content. On the other hand EX-IM process promotes the alignment of the fibers along the flow direction, and thus limits their reinforcing capability with respect to flexural testing. This is the reason why the relative improvement observed for EX-CM composites is higher than that shown by EX-IM samples. Therefore, CM leads to lower strength but higher degree of improvement with respect to the strength of the neat polymer compared to IM. For example, addition of 20 wt.% VGCF leads to strength increase of neat PLA by 10% and 30% when IM and CM are used, respectively.

In general, the smaller the filler, the larger the surface area is and thus the larger the interface available for interactions with the polymer matrix. Both fillers lack functional groups which could favor the interactions with PLA so there is no chemical affinity between any of the fillers and the matrix. This means that there are voids and imperfect contact at the filler/polymer interface. A phenomenon that is most dominant in case of xGnP which has the smallest size and highest surface area.

The effect of nanofiller synergy and processing method on the flexural properties of PLA composites with total filler content of 10 wt.%, at various filler ratios, is shown in Fig. 7. No significant synergy is observed and the general trend is that VGCFs dominate the strength which increases with VGCF content whereas the xGnPs stongly affect the modulus.

The effect of compounding method on the flexural properties of VGCF/PLA and xGnP/PLA composites is presented in Table 1. The results are nonconclusive, however, compounding by solution method seems to induce larger improvement in mechanical properties at higher filler loadings. On the other hand, for lower filler loadings and for neat PLA, melt extrusion is a preferable method. It is expected that the

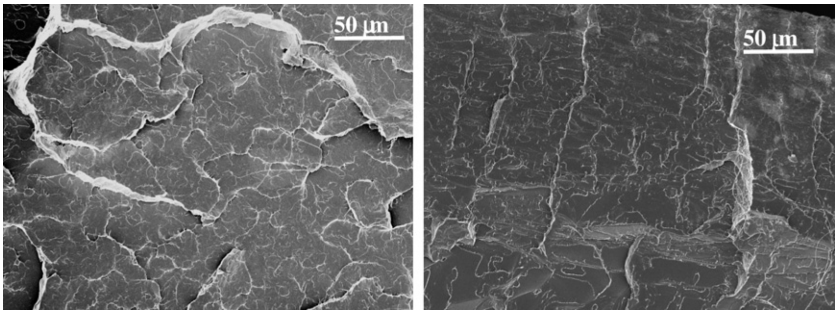

Fig. 6 – FESEM images of the fracture surface of neat PLA specimens made by (a) EX-IM and (b) EX-CM.

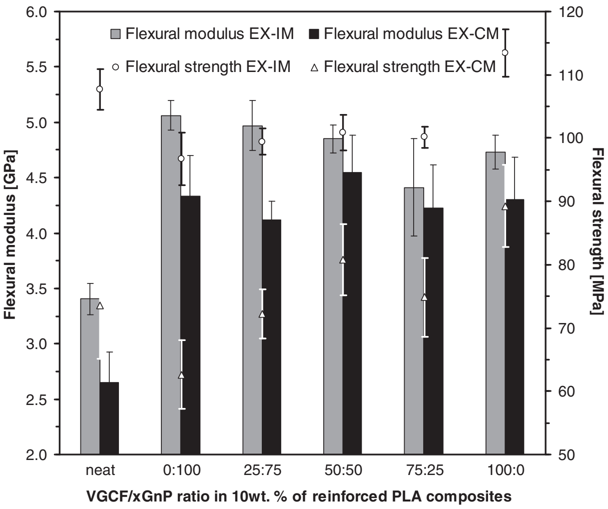

Fig. 7 – Effect of filler synergy and processing on flexural properties of PLA composites with total filler content of 10 wt.%.

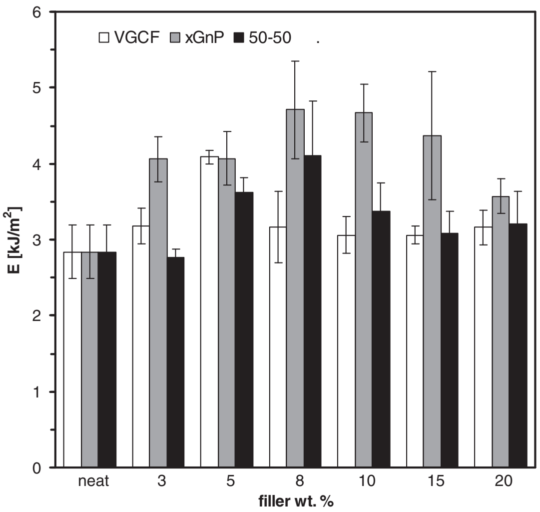

Fig. 8 – Effect of filler type and content on Charpy specific energy of PLA composites made by EX-IM.

compounding method will strongly affect the electrical conductivity of these composites.

3.2. *Impact resistance*

The specific energy absorbed by the VGCF/PLA and xGnP/PLA composites before they fracture under impact is shown in Fig. 8 as a function of the filler loading. The effect of filler synergy on the impact energy is also reported for composites containing VGCF/xGnP weight ratio equal to one (indicated as 50/50 in the figure). As shown, addition of VGCF improves the impact energy only for VGCF content up to 5 wt.%. Addition of xGnP improves the impact energy for all xGnP contents used in the study with the largest increase in strength, by more than 65%, observed for xGnP contents of 8 and 10 wt.%. Upon further addition of filler, homogeneous dispersion becomes challenging and filler agglomeration is unavoidable leading to decrease in impact energy. It is noted that an optimum filler content at about 8 wt.% exists when both fillers are simultaneously added at which the maximum improvement in impact energy in observed. No synergistic effect due to addition of both fillers on the impact strength is observed.

3.3. *Viscoelastic properties and softening temperature*

The temperature dependence of the storage (E') and loss (E'') moduli of PLA and representative VGCF/PLA and xGnP/PLA composites made by EX-CM are shown inFig. 9a and b, respectively. The storage modulus gradually decreases with temperature for temperatures below the glass transition temperature, T_g. A drastic drop of modulus values by three orders of magnitude (down to 4–6 MPa) is observed after T_g indicating material transition from the glassy to the rubbery state. This can be also considered as a clear indication that almost completely amorphous materials are produced under the adopted processing conditions. In fact, for semicrystalline PLA a much lower E' reduction is generally induced when the temperature is raised up to 100 °C [21]. Moreover, the tanδ peak values summarized in Table 2 are characteristic of almost fully-amorphous compression-molded PLA [22]. The same trend is observed for the neat PLA and the composite systems. Addition of filler increases the storage modulus of the PLA and enables the composites to be used at higher temperatures compared to the performance temperature of neat PLA.

The loss modulus is also increasing with filler content for both fillers used. This increase is a result of the mechanical loss generated in the interface regions due to confinement of the polymer chains. Furthermore, the T_g, calculated as the temperature of the tanδ peak, is also increasing with filler content.

The storage modulus at ambient temperature, the tanδ peak and T_g values (corresponding to tanδ peak) for VGCF/PLA and xGnP/PLA composites as a function of the filler content and the processing methods are presented in Table 2. The

Table 1 – Flexural properties of PLA composites as a function of the filler type and content and compounding method used.

Filler type	wt.%	EX-CM modulus (GPa)	EX-CM strength (MPa)	SO-CM modulus (GPa)	SO-CM strength (MPa)
None	0	2.65 ± 0.28	73.6 ± 8.4	2.38 ± 0.37	63.2 ± 2.9
xGnP	5	4.05 ± 0.58	83.8 ± 11.6	3.42 ± 0.33	65.5 ± 4.4
	10	4.33 ± 0.37	62.6 ± 5.5	4.96 ± 0.35	88.9 ± 3.9
VGCF	5	3.88 ± 0.30	90.4 ± 10.9	3.59 ± 0.29	75.0 ± 3.7
	10	4.30 ± 0.39	89.2 ± 6.5	5.06 ± 0.37	93.6 ± 4.1

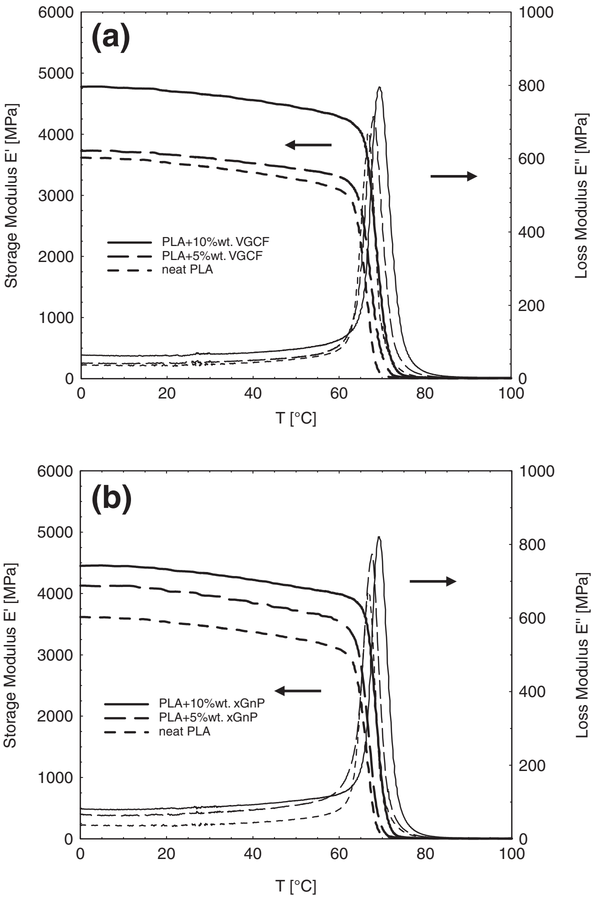

Fig. 9 – Storage (E') and loss (E'') modulus as a function of temperature for (a) VGCF/PLA and (b) xGnP/PLA composites made by EX-CM.

storage modulus of neat PLA increases with addition of fillers for all three processing methods studied, with the highest increase observed in case of xGnP. This is expected because upon addition of fillers the composites become more elastic and less energy is dissipated by the random motion of the polymer chains due to confinement of the polymer molecules by the filler. It is noted that the trend in the storage modulus of the PLA composites made by EX-CM and EX-IM is similar to the trend in flexural modulus of these composites reported in Fig. 4.

As shown in Table 2, both the neat PLA and the PLA composites processed by EX-IM exhibit significant lower storage modulus compared to their counterparts processed by SO-CM and EX-CM. This could be attributed to differences in the polymer's compaction and free volume (physical aging) state induced by the different processing methods.

The effect of processing method on T_g is more dramatic that the effect caused by addition of the fillers. Irrelevant of the method employed to make the composites, addition of fillers increases the T_g indicating that higher temperature (more energy) is required before the polymer chains can freely flow. This means that the rubbery regime has shifted to higher temperatures due to the presence of the fillers that pin the polymer chains. Neat PLA and corresponding composites made by SO-CM exhibit the lowest T_g and tanδ peak values followed by composites made by EX-CM and finally those made by EX-IM. The basic differences of the three methods are the (i) thermal history the polymer exhibits which relates to its physical aging and (ii) order/alignment of both the polymer chains and the filler with the most random distribution observed in SO-CM, followed by EX-CM and finally EX-IM where the fillers are aligned along the injection molding direction. Also the presence of aggregates in the SO-CM indicate that the polymer–filler interface is limited so the polymer chains are not as pinned as in the other cases and flow at lower temperatures (T_g). The tanδ peak values are not substantially affected by the presence of xGnP, thus confirming the hypothesis of poor filler–matrix interactions. On the other hand, tanδ peak (i.e., chain mobility) is markedly reduced by addition of VGCF.

Vicat softening temperature is defined as the temperature at which a flat ended probe of 1 mm^2 circular cross section penetrates the specimen to a depth of 1 mm under a specific load using a selected temperature ramp. This parameter is generally adopted to establish the service temperature of thermoplastic polymers. The Vicat softening point is nothing but a temperature at which the modulus has reached a particular level. So the Vicat softening point is a well-defined point in the modulus-temperature diagram, being related to the fundamental properties of the material [23]. Fig. 10 reports Vicat temperature as a function of the filler type and content for EX-IM composites. As shown, the Vicat temperature noticeably increases with the filler content. This effect is more evident in VGCF/PLA composites rather than xGnP/PLA composites.

3.4. *Electrical conductivity*

Carbon materials, when used as reinforcements in polymers, can induce electrical and thermal conductivity in addition to enhancing the mechanical and thermo-mechanical

Table 2 – Storage modulus at 25 °C, and tanδ peak and temperature (T_g) as a function of filler type and content, and of the processing method used.

Filler type	wt.%	SO-CM E' (GPa)	EX-CM E' (GPa)	EX-IM E' (GPa)	SO-CM tanδ peak	EX-CM tanδ peak	EX-IM tanδ peak	SO-CM T_g (°C)	EX-CM T_g (°C)	EX-IM T_g (°C)
None	0	3.26	3.50	2.10	1.70	2.51	2.85	67.9	69.8	75.7
xGnP	5	3.63	4.02	2.94	1.71	2.58	2.75	68.9	71.4	76.3
	10	5.62	4.36	3.36	1.93	2.52	2.29	71.3	73.8	77.6
VGCF	5	3.48	3.63	2.60	1.56	1.96	2.10	70.5	72.4	77.3
	10	3.43	4.68	2.79	0.91	1.81	1.67	71.8	74.8	78.4

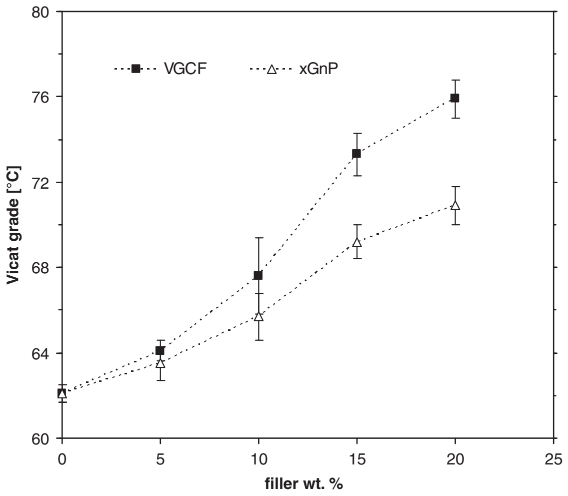

Fig. 10 – Vicat softening temperature as a function of filler type and content for composites made by EX-IM.

properties of the matrix. The minimum amount of filler required to form a conductive network within the polymer is called percolation threshold. Ideally, percolation threshold should be as low as possible in order to keep the processing simple (relatively low viscosity of the melt) and the cost low.

The surface resistivity of VGCF/PLA and xGnP/PLA composites, as a function of the filler content and molding process used to make the composites, is shown in Figs. 11 and 12, respectively. In case of EX-CM composites, the resistivity decreases with filler content with a dramatic drop observed after percolation. In fact, a percolation threshold is observed between 5 and 7 wt.%, with a resistivity decrease by 4–5 orders of magnitude. xGnP/PLA composites prepared by EX-CM exhibit a higher percolation threshold between 10 and 15 wt.% with the corresponding resistivity being 3–4 orders of magnitude lower than that of unfilled PLA.

On the other hand, neither VGCF/PLA nor xGnP/PLA composites prepared by EX-IM exhibit a clear percolation threshold. In case of VGCF/PLA composites it takes addition of 20 wt.% of VGCF before the resistivity reduces by three orders of magnitude. In case of xGnP/PLA composites the resistivity is hardly reduced by one order of magnitude even with addition of 20 wt.% xGnP indicating that the percolation threshold is even higher than 20 wt.%.

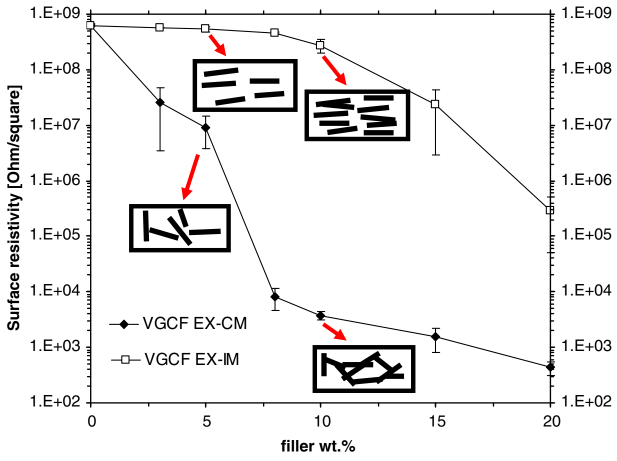

Fig. 11 – Surface resistivity of VGCF/PLA composites as made by EX-CM and EX-IM.

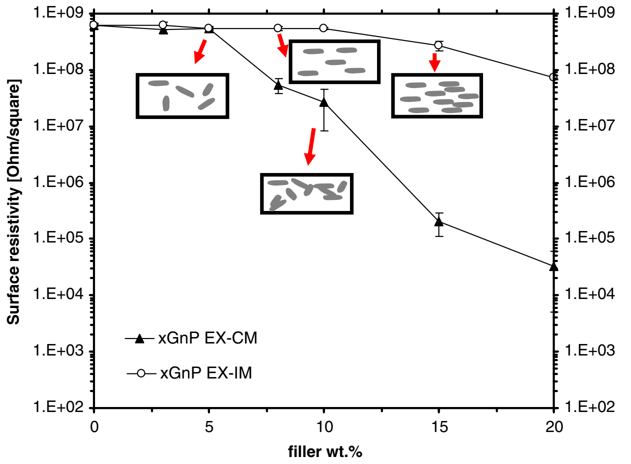

Fig. 12 – Surface resistivity of xGnP/PLA composites made by EX-CM and EX-IM.

The main reason why the composites made by EX-CM exhibit significantly lower percolation threshold and lower surface resistivity compared to the corresponding composites made by EX-IM could be the following. The fillers orient along the injection molding direction and only at higher filler contents they will start contacting each other forming a conductive network within the polymer, thus decreasing the electrical resistivity in the injection molding direction which is the direction along which the conductivity is measured. On the other hand, the random filler orientation during compression molding facilitates the formation of the network at much lower filler contents as shown also in the schematics presented in Figs. 11 and 12. Finally, it is noted that VGCF reinforced composites exhibit lower percolation threshold and lower resistivity than their xGnP counterparts because, due to their one-dimensional shape and high aspect ratio, it is easier to form a conductive network. Similar results have been also reported for other polymers, such as poypropylene, polycarbonate and ABS, filled with aluminum flakes [24].

In order to understand the effect of the compounding method on the percolation threshold and resistivity of the PLA composites, VGCF/PLA and xGnP/PLA composites were made using melt mixing (EX) and polymer dissolution (SO) methods followed by compression molding. CM is chosen as the molding method because it leads to composites with lower percolation and lower conductivity compared to IM, as previously presented. The results are shown in Fig. 13.

As indicated, polymer dissolution results in significantly lower resistivity for both composite types. The effect of the compounding method is more obvious in case of VGCF/PLA composites which, as discussed previously, when made by EX-CM have a percolation threshold at around 5 wt.%. SO compounding reduces the resistivity of VGCF/PLA composites compared to that of neat PLA by 6 and 7 orders of magnitude for 5 and 10 wt.% VGCF, respectively. The corresponding

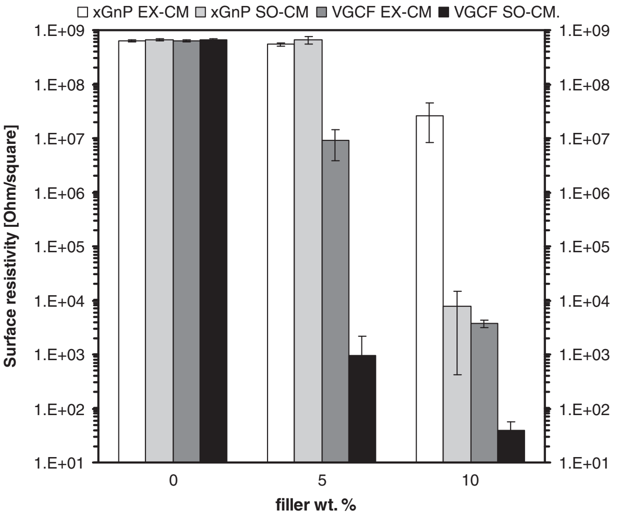

Fig. 13 – Surface resistivity of PLA composites as a function of filler type and content and of the compounding method used.

reduction in resistivity caused by EX compounding is 2 and 5 orders of magnitude, which is significantly smaller. It is also expected that SO will result in VGCF composites with percolation threshold lower than 5 wt.%.

The same trend is observed for xGnP/PLA composites but the effect of compounding method on the resistivity is only obvious at 10 wt.% of xGnP because the percolation threshold is higher than 5 wt.% as discussed previously. SO results in resistivity that is four orders of magnitude lower than the resistivity of 10 wt.% xGnP composite made by EX.

Considering that, as reported in Table 1, there is no significant effect of the compounding method on the flexural strength and modulus of VGCF/PLA and xGnP/PLA composites SO compounding followed by compression molding should be used if composites with low percolation threshold and low surface resistivity are required.

In conclusion, composites made by EX-IM exhibit highest percolation threshold and resistivity followed by those made by EX-CM and finally by those made by SO-CM. Filler alignment along the injection molding direction is the reason behind the high percolation threshold of EX-IM composites as discussed previously. The basic difference in resistivity between composites made by EX-CM and SO-CM can be attributed to the following reasons: (i) melt mixing in the extruder may result in a reduction of the fillers' aspect ratio and thus increase of percolation threshold and (ii) in SO dispersion no shear stresses are applied and the fillers probably retain the initial dimension (aspect ratio) and aggregation state. The SO process may favor some clustering of the VGCF and a segregated distribution that could drastically increase the electrical conductivity after the percolation threshold, as clearly reported for metal-filled polymers [25].

The above remarks are reflected in the representative SEM images of 3 wt.% VGCF/PLA composites made by EX-IM, EX-CM and SO-CM shown inFig. 14a–c, respectively. The observed fracture surfaces were obtained by cryofracture of the samples in liquid nitrogen. As indicating in Fig. 14a, most of the VGCFs are pointing out of the fracture plane indicating alignment along the injection molding direction whereas, a more random fiber distribution is observed in composites made by EX-CM shown in Fig. 14b. Finally, the formation of a continuous fiber network, with fibers that are significantly longer than those shown in Fig. 14b is shown in Fig. 14c. Moreover, the clusters of segregated fillers connected by long fibers observed for VGCF/PLA composites processed by SO-CM, shown in Fig. 14d, can explain the lower resistivity values above the percolation threshold.

The effect of filler synergy on the surface resistivity of VGCF/xGnP/PLA composites made by EX-CM with a total filler amount of 10 wt.% was also studied. The results are shown in Fig. 15. Schematics indicating the filler dispersion and formation of a conductive network within the polymer are also shown. As expected, the higher the VGCF content the lower the resistivity with the lowest value observed for 10 wt.% VGCF and 0 wt.% xGnP. However, if the overall performance of the composites is considered including flexural strength and modulus and impact energy, presented in Figs. 7 and 8, respectively, a VGCF/xGnP/PLA composite with a total filler loading of 10 wt.% containing VGCF/xGnP at a ratio of 1, indicated as 50:50 is the optimum composite. Synergy due to addition of both fillers is expected to be more dominant at filler contents higher than 10 wt.% that is above the xGnP's percolation threshold.

It is noted that there is a trade off between enhancing flexural strength and inducing electrical conductivity in a composite system. Nano-size particles and homogeneous dispersion of individual fillers can lead to significant enhancement of the strength assuming perfect contact at the polymer–filler interface. Induction of electrical conductivity requires the formation of a continuous network. This is easier accomplished if larger particles or really high aspect ratio fillers are used. The fillers need to touch or be very close to each other, to allow electron tunneling, which means that the chances of aggregation are increased and thus flexural strength will not improve as much. As shown, regardless of the filler type and the manufacturing process, an increase of the filler content enhances both the dimensional stability (stiffness, Vicat grade) and the electrical conductivity. On the other hand, it can be noticed how the potential of both nanofiller in increasing the mechanical and the flexural properties of the PLA strongly depends on the properties of the matrix itself. In fact, neat PLA prepared by SO-CM present lower elastic modulus and stress at break with respect to the corresponding matrix prepared by EX-IM and EX-CM. The addition of such nanofillers in a more compliant matrix favors filler–filler interactions and a remarkable increase of both the flexural properties and of the electrical conductivity even at low filler contents.

Finally, it is interesting to observe that, while no synergism between nanofillers was detected in flexural tests, combination of the fillers promotes a further decrease of surface resistivity. This is due to the fact that the formation of a three dimensional conductive network within the matrix plays a key role in increasing electrical conductivity values, while mechanical properties are only marginally affected by filler networking.

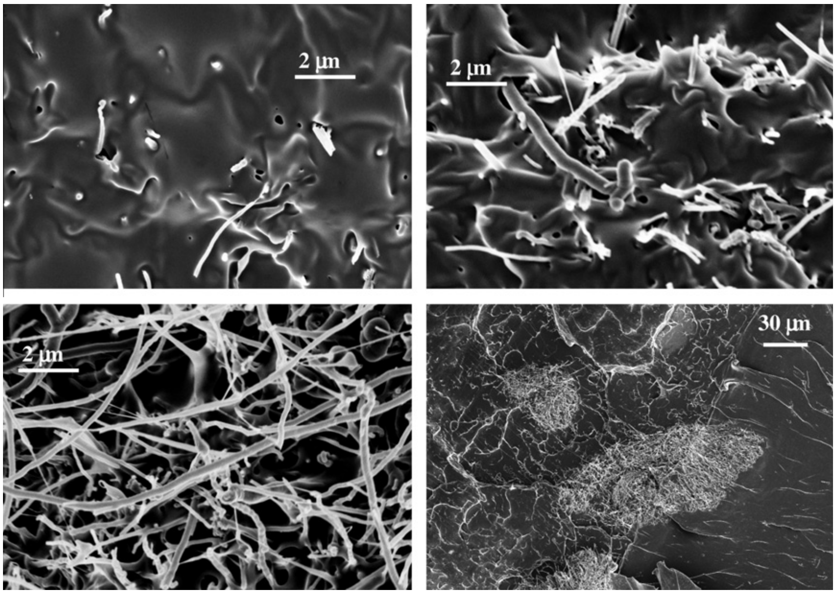

Fig. 14 – FESEM images of the fracture surface of 3 wt.% VGCF/PLA composites made by (a) EX-IM, (b) EX-CM, (c) SO-CM and (d) low magnification of SO-CM showing aggregates of VGCFs.

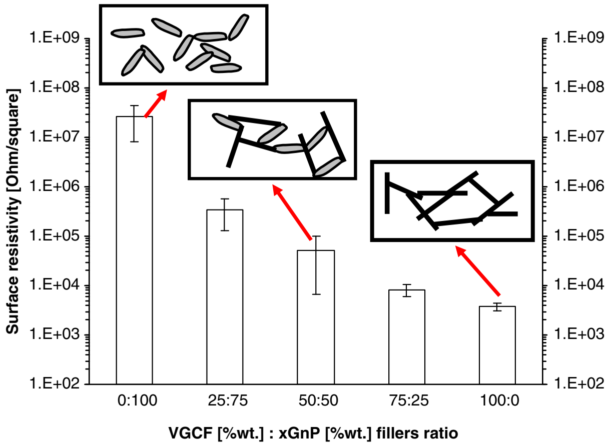

Fig. 15 – Effect of filler synergy on surface resistivity of PLA composites made by EX-CM with a total filler amount of 10 wt.%.

4. Conclusions

VGCF/PLA and xGnP/PLA composites with filler content from 0 to 20 wt.% were made using two different compounding methods, melt mixing and polymer dissolution, followed by either injection or compression molding. The two fillers were also combined in order to explore possible synergistic actions. The study demonstrates how the mechanical, viscoelastic and electrical properties of the biodegrable PLA matrix can be tuned by a proper choice of filler type/content and processing conditions.

The xGnP/PLA composites made by EX-IM exhibited the highest flexural modulus and impact resistance but were not electrically conductive even at 20 wt.% of xGnP due to alignment along the injection molding direction. When compression molding was used instead of injection molding, the electrically resistivity of the xGnP/PLA composites reduced significantly and the storage modulus increased with no decrease in the flexural modulus. However, EX-CM led to decrease of the flexural strength. xGnP/PLA composites made by SO-CM exhibited mechanical and viscoelastic properties similar and significantly higher electrical conductivity compared to composites made by EX-CM.

The effect of processing method on the properties of VGCF/PLA composites was similar to that observed for the xGnP/PLA composites with the basic difference that the VGCF/PLA composites exhibited higher flexural strength, Vicat softening point and electrical conductivity compared to the xGnP/PLA composites but lower flexural modulus. The presence of voids at the xGnP/PLA interface observed by SEM is the reason for the low flexural strength of the xGnP/PLA composites whereas the tubular shape and high aspect ratio of VGCF are responsible for the lower percolation threshold and surface resistivity observed for the VGCF/PLA composites.

Significant effect of the processing method on the storage modulus and T_g of the neat PLA and the PLA composites was observed with the SO-CM that lead to the highest storage modulus and lowest T_g. Finally, VGCF/xGnP/PLA composite made by EX-CM with a total filler loading of ~10 wt.% containing VGCF/xGnP at a ratio of 1, was determined as the composite with the best combination of filler type/content and processing method considering the overall performance including flexural strength and modulus, impact energy and electrical conductivity.

Considering that VGCF revealed more effective in increasing the strength and the thermal stability of the material, this nanofiller can be very promising for applications where good dimensional stability at elevated temperatures is required, such as packaging materials. Furthermore, the synergistic effect between the nanofillers in decreasing surface resistivity of the specimens can find application for production of biodegradable composites for EMI (electromagnetic interference) shielding properties, a feature highly required for plastic housings of electronics. Finally these biodegradable composites can be used in automotive industry in the exterior automotive body, i.e., rear bumper or mirror housing and interior panels eliminating the need of a primer during electrostatic painting.

Acknowledgments

The authors would like to thank Professors G. Yushin and D. Yao from Georgia Institute of Technology for allowing access to the electrical conductivity apparatus, and hydraulic press, respectively. The helpful discussions with Mr. R. Brown, Dr. A. Magasinski and Mr. C. Petersburg also from Georgia Institute of Technology are acknowledged. Finally, special thanks to Mr. L. Moschini from University of Trento for helping with the FESEM study.

REFERENCES

[1] Vaia RA. Polymer nanocomposites open a new dimension for plastics and composites. AMPTIAC Newsl 2003;17:8–11.
[2] Vaia RA, Jandt KD, Kramer EJ, Giannelis EP. Microstructural evolution of melt intercalated polymer-organically modified layered silicates nanocomposites. Chem Mater 1996;8(11):2628–35.
[3] Kato M, Usuki A, Okada A. Synthesis of polypropylene oligomer–clay intercalation compounds. J Appl Polym Sci 1997;66(9):1781–5.
[4] Kawasumi M, Hasegawa N, Kato M, Usuki A, Okada A. Preparation and mechanical properties of polypropylene–clay hybrids. Macromolecules 1997;30(20):6333–8.
[5] Yasmin A, Abot JL, Daniel IM. Processing of clay/epoxy nanocomposites by shear mixing. Scripta Mater 2003;49(1):81–6.
[6] Kalaitzidou K, Fukushima H, Drzal LT. Mechanical properties and morphological characterization of exfoliated graphite–polypropylene nanocomposites. Compos Part A Appl Sci Manuf 2007;38(7):1675–82.
[7] Messersmith PB, Giannelis EP. Polymer-layered silicate nanocomposites: in situ intercalative polymerization of epsilon-caprolactone in layered silicates. Chem Mater 1993;5(8):1064–6.
[8] Krishnamoorti R, Vaia RA, Giannelis EP. Structure and dynamics of polymer-layered silicate nanocomposites. Chem Mater 1996;8(8):1728–34.
[9] Lunt J. Large-scale production, properties and commercial applications of polylactic acid polymers. Polym Degrad Stabil 1998;59(1–3):145–52.
[10] Martin O, Avérous L. Poly(lactic acid): plasticization and properties of biodegradable multiphase systems. Polymer 2001;42(14):6209–19.
[11] Drumright RE, Gruber PR, Henton DE. Polylactic acid technology. Adv Mater 2000;12(23):1841–6.
[12] Tsuji H, Ikada Y. Properties and morphologies of poly(-lactide): 1. annealing condition effects on properties and morphologies of poly(-lactide). Polymer 1995;36(14):2709–16.
[13] Fambri L, Pegoretti A, Fenner R, Incardona SD, Migliaresi C. Biodegradable fibres of poly(-lactic acid) produced by melt spinning. Polymer 1997;38(1):79–85.
[14] Yoon JT, Lee SC, Jeong YG. Effects of grafted chain length on mechanical and electrical properties of nanocomposites containing polylactide-grafted carbon nanotubes. Compos Sci Technol 2010;70(5):776–82.
[15] Villmow T, Pötschke P, Pegel S, Häussler L, Kretzschmar B. Influence of twin-screw extrusion conditions on the dispersion of multi-walled carbon nanotubes in a poly(lactic acid) matrix. Polymer 2008;49(16):3500–9.
[16] Murariu M, Dechief AL, Bonnaud L, Paint Y, Gallos A, Fontaine G, et al. The production and properties of polylactide composites filled with expanded graphite. Polym Degrad Stabil 2010;95(5):889–900.
[17] Kim HS, Kwon HI, Kwon SM, Yun YS, Yoon JS, Jin HJ. Electrical and mechanical properties of poly(l-lactide)/carbon nanotubes/clay nanocomposites. J Nanosci Nanotechnol 2010;10(5):3576–80.
[18] Miloaga DG, Hosein HAA, Rich MJ, Kjoller K, Drzal LT. Scanning probe thermal analysis of polylactic acid/exfoliated graphite nanoplatelet (xGnP (™)) nanocomposites. J Biobased Mater Bioenergy 2008;2(1):78–84.
[19] Du JH, Bai J, Cheng HM. The present status and key problems of carbon nanotube based polymer composites. Express Polym Lett 2007;1(5):253–73.
[20] Kalaitzidou K, Fukushima H, Drzal LT. Multifunctional polypropylene composites produced by incorporation of exfoliated graphite nanoplatelets. Carbon 2007;45(7):1446–52.
[21] Pegoretti A, Fambri L, Migliaresi C. In vitro degradation of poly(L-lactic acid) fibers produced by melt spinning. J Appl Polym Sci 1997;64(2):213–23.
[22] Migliaresi C, Cohn D, Delollis A, Fambri L. Dynamic mechanical and calorimetric analysis of compression-molded PLLA of different molecular weights Effect of thermal treatments. J Appl Polym Sci 1991;43(1):83–95.
[23] Namhata SP, Santolini L, Locati G. Rationalization of Vicat softening point measurements. Polym Test 1990;9(2):75–89.
[24] Bigg DM. Electrical properties of metal-filled polymer composites. In: Bhattacharya SK, editor. Metal-filled polymers. New York: Marcel Dekker Inc.; 1986. p. 165–226.
[25] Kusy RP. Applications. In: Bhattacharya SK, editor. Metal-filled polymers. New York: Marcel Dekker Inc.; 1986. p. 1–142.